Optical Engineering

SPIEDigitalLibrary.org/oe

Autoexposure for three-dimensional shape measurement using a digital-light-processing projector

Laura Ekstrand
Song Zhang

Autoexposure for three-dimensional shape measurement using a digital-light-processing projector

Laura Ekstrand
Song Zhang
Iowa State University
Department of Mechanical Engineering
Ames, Iowa 50011
E-mail: song@iastate.edu

Abstract. Automatically adapting the camera exposure time is crucial for industrial applications where minimum human intervention is usually desirable. However, it is very challenging to realize such a capability for a conventional fringe projection system where only a finite increment of the exposure time is allowed due to its digital fringe generation nature. We study the generation of sinusoidal fringe patterns by properly defocusing binary ones, which permits the use of an arbitrary exposure time. This provides the potential to adapt the exposure time automatically. We present the principle of an automatic exposure technique and show some experimental results.
[DOI: 10.1117/1.3662387]

Subject terms: phase shifting; autoexposure; three-dimensional; defocusing; digital fringe projection.

Paper 110933PR received Aug. 4, 2011; revised manuscript received Oct. 19, 2011; accepted for publication Oct. 26, 2011; published online Nov. 29, 2011.

1 Introduction

Automatically adapting the camera exposure based on the surface reflectivity of a measured object is crucial for industrial applications where minimum human intervention is usually desirable, and three-dimensional (3-D) shape measurement with digital fringe projection techniques is not an exception. However, it is very challenging to realize such a capability for a conventional fringe projection system.

There are basically five approaches to changing the intensity of the camera image in a fringe projection system: (*i*) Adjust projector aperture, (*ii*) adjust camera aperture, (*iii*) adjust projected fringe intensity, (*iv*) adjust camera gain, and (*v*) adjust camera exposure time. These methods can be classified into two categories: those requiring manual input (i.e., *i* and *ii*) and those that can be performed automatically. Typically, the best method for adjusting image exposure to acquire high-quality fringe patterns is to manually adjust one of the lens apertures. However, manual adjustments can cause undesired motion between system components that changes the system calibration. Therefore, development of a method that can automatically adjust image exposure is vital for high-precision 3-D shape measurement. Adjusting the projected fringe pattern intensity is one of the options. This technique has been proposed to handle shiny object measurement.[1] However, the fringe pattern is typically restricted to 8 bits (256 grayscale values). Moreover, changing the maximum grayscale value usually affects the signal-to-noise ratio (SNR) of the measurement because the fringe contrast changes. In general, sacrificing fringe contrast is not desirable. Likewise, it is also usually not desirable to change the camera gain because the SNR also changes accordingly.

Therefore, it seems that adjusting the camera exposure time is the best option. However, for conventional sinusoidal fringe patterns displayed on a digital-light-processing (DLP) projector, the camera exposure time cannot be arbitrarily chosen beacuse the projector relies on time modulation for the generation of grayscale values between 0 and 255. To precisely capture the projected grayscale values, the projector and camera must be precisely synchronized, and the smallest step to adjust the camera exposure time is its channel projection time (e.g., $\Delta t = 8.33$ ms for a 120-Hz projector).[2] This step size is typically one to two orders of magnitude larger than the step size needed for practical exposure adjustment.

In this research, we propose to use the projector-defocusing technique[3] to circumvent the finite exposure time increment problem. This new technique for 3-D shape measurement requires only binary structured patterns to realize conventional phase-shifting algorithms; the sinusoidal fringe patterns are realized by properly defocusing the projector. To increase the depth range of this technique, we will use binary patterns generated by optimal pulse width modulation (OPWM) rather than simple square waves. OPWM modifies a square wave pattern such that undesired harmonics that would decrease the depth range for 3-D measurement are removed from the defocused result.[4] Because this defocusing technique coincides with the operation mechanism of the DLP projector, it permits the use of an arbitrary exposure time for 3-D shape measurement.[5] And because an arbitrary exposure time can be used, this new technique provides the opportunity to develop an automatic exposure adjustment strategy for a digital fringe projection system.

This paper will present a 3-D shape measurement system that could change its exposure time automatically according to the surface reflectivity of the measured object. The system uses a strategy that analyzes images of the object under uniform pure white light at several exposure times to determine the object's surface reflectivity; the strategy then predicts an exposure time for the object that effectively controls the percentage of saturated pixels allowed in subsequent images. We have found that by controlling the exposure time automatically in this manner, high-quality 3-D shape measurements can always be achieved for any type of diffuse object. This paper will present the principle of this technique

0091-3286/2011/$25.00 © 2011 SPIE

in Sec. 2 and show some experimental results in Sec. 3. Section 4 will discuss additional considerations. Finally, Sec. 5 will summarize this paper.

2 Principles

2.1 *Three-Step Phase-Shifting Technique*

Phase-shifting methods are widely used in optical metrology because of their speed and accuracy.[6] Over the years, numerous phase-shifting algorithms have been developed, including three-step, four-step, double three-step, etc. In this research, we use a three-step phase-shifting algorithm to find the phase value. Three fringe images with a phase shift of $2\pi/3$ can be written as follows

$$I_1(x, y) = I'(x, y) + I''(x, y)\cos(\phi - 2\pi/3), \quad (1)$$

$$I_2(x, y) = I'(x, y) + I''(x, y)\cos(\phi), \quad (2)$$

$$I_3(x, y) = I'(x, y) + I''(x, y)\cos(\phi + 2\pi/3). \quad (3)$$

In Eqs. (1)–(3), $I'(x, y)$ is the average intensity, $I''(x, y)$ the intensity modulation, and $\phi(x, y)$ the phase to be computed. From Eqs (1)–(3), we can obtain the phase

$$\phi(x, y) = \tan^{-1}[\sqrt{3}(I_1 - I_3)/(2I_2 - I_1 - I_3)]. \quad (4)$$

Equation (4) provides the $\phi(x, y)$ value, ranging from $-\pi$ to $+\pi$ with 2π discontinuities, which is usually called the wrapped phase. The 2π phase discontinuities can be removed to obtain a continuous phase map by adopting a phase-unwrapping algorithm.[7] Once the continuous phase map is obtained, the 3-D shape can be recovered from the phase through calibration.[8]

2.2 *Digital-Light-Processing Fundamentals*

The core of the digital-light-processing projector is the digital micromirror device (DMD). Each micromirror can rotate between $+\theta_L$ (ON) and $-\theta_L$ (OFF). The grayscale value of each pixel is realized by controlling the ON time ratio: 0% ON time represents 0, 50% ON time means 128, and 100% ON time is 255. Therefore, a DLP projector produces a grayscale value by time modulation.[9]

We have carried out a simple experiment to verify the time modulation behavior of the DLP projector used in our system, the Logic PD DLP LightCommander development kit. In this experiment, we connected a photodiode (model: Thorlabs FDS100) with a resistor (30 kΩ) to sense the output light of the projector. An oscilloscope (Tektronix TDS2024B) was used to monitor the voltage of the photodiode system as the projector projected uniform grayscale images at values of 255, 128, 64, and 0. Figure 1 shows the resulting oscilloscope output. In Figs. 1(a) and 1(d), the light level from the projector appears relatively constant at a high level and low level, respectively. At a grayscale value of 128, as shown in Fig. 1(b), the light level alternates between low and high, remaining at each level for approximately equal amounts of time. At a grayscale value of 64, the light level again alternates between the two levels, but it only jumps to the high level for about one-quarter of the time. These experiments showed that if the projected image contains grayscale values between 0 and 255, as sinusoidal fringe patterns do, the whole projection period must be captured to image the correct pattern. Therefore, to correctly capture a conventional sinusoidal fringe pattern projected by a 60-Hz DLP projector for 3-D shape measurement, the camera exposure time must be a multiple of 1/60 s. This is certainly not desirable when the flexibility of controlling exposure time is required. In contrast, if the projected image contains only 0s and/or 255s, then each DLP micromirror remains stationary between refreshes, and thus, any partial time segment can represent the whole projected signal. Therefore, an arbitrary camera exposure time can be utilized to capture the projected image, as has been previously verified.[5]

2.3 *Sinusoidal Fringe Pattern Generation by Defocusing*

As aforementioned, if the DMD is fed with 0 or 255, it will retain its status (without flipping ON/OFF) during the period of channel projection. Therefore, if binary (0s and 255s) instead of sinusoidal structured patterns are used, it permits the use of an arbitrary exposure time for the camera. However, to perform 3-D shape measurement with a phase-shifting method, sinusoidal fringe patterns are required.

Our recent study showed that by properly defocusing a binary structured pattern, a pseudosinusoidal one can be generated,[3] which is similar to the Ronchi grating defocusing method proposed by Su et al.[10] Figure 2 shows some typical results when the projector is defocused to different degrees while the camera is in focus. The pattern employed here is a basic set of black-and-white stripes referred to as a squared binary pattern (SBM). Figure 2 shows that, as the projector becomes increasingly defocused, the binary structured pattern becomes increasingly distorted. Figure 2(a) shows the result when the projector is in focus: clear binary structures on the image. As the degree of defocusing increases, the binary structures become less and less clear and the sinusoidal ones become more and more obvious. However, if the projector is defocused too much, then the sinusoidal structures start diminishing, as indicated in Fig. 2(f). This experiment

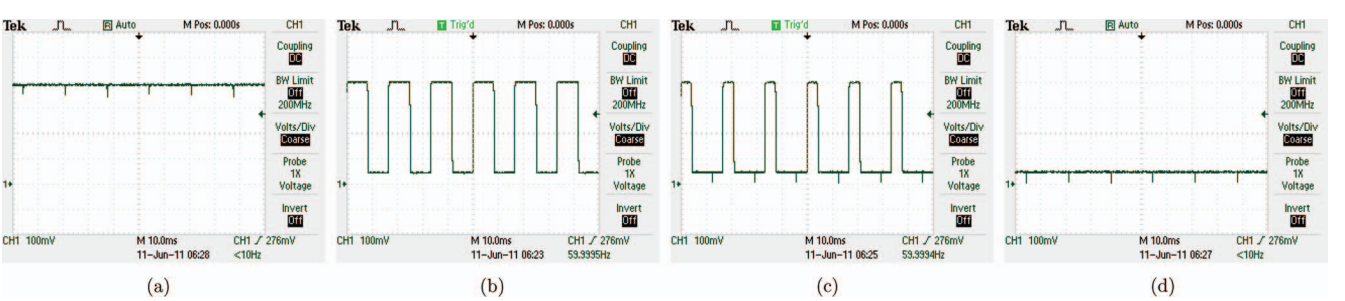

Fig. 1 Examples of DLP time modulation for images with different uniform grayscale values: (a) 255, (b) 128, (c) 64, and (d) 0.

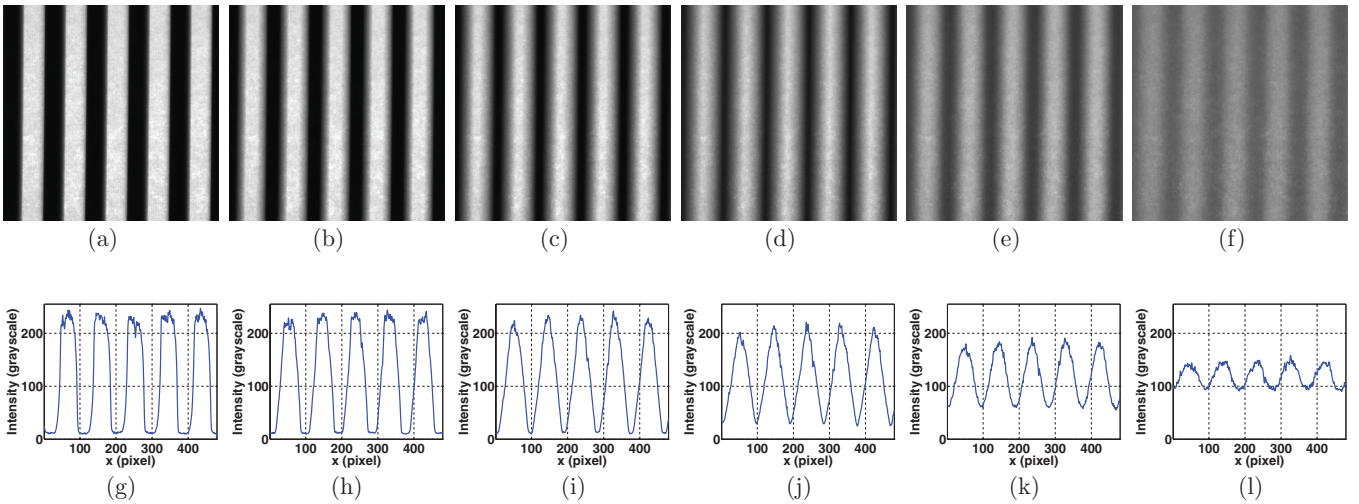

Fig. 2 Example of sinusoidal fringe generation by defocusing a binary structured pattern: (a) Shows the result when the projector is in focus; (b–f) show the result when the projector is increasingly defocused, and (g–l) illustrate the 240th-row cross section of the corresponding image above.

indicates that a pseudosinusoidal fringe pattern can indeed be generated by properly defocusing a binary structured pattern.

However, this seemingly sinusoidal fringe pattern retains some of its binary structure in the form of harmonics beyond the fundamental sinusoidal frequency. Some of these harmonics induce errors in the results that limit the depth range for accurate 3-D measurement. An alternative approach to the defocusing technique uses fringe patterns generated by OPWM, which produces binary fringe patterns by selectively removing regions of the square wave of SBM that would generate the undesired harmonics after defocusing.[4] This technique is used in the field of electrical engineering to generate sinusoidal waveforms.[11] Figure 3 shows an SBM pattern in comparison to an OPWM pattern, illustrating the shifting of columns that takes place during the removal of selected harmonics. Indeed, Fig. 3(b) appears more sinusoidal even prior to defocusing. Therefore, defocused OPWM patterns offer a binary alternative to sinusoidal patterns for phase shifting while still allowing an arbitrary camera exposure time.

2.4 *Automatic Exposure Adaption Framework*

Given an arbitrary object with an unknown surface reflectivity, it is very difficult to determine the optimal exposure time. Therefore, the first step of this framework must be an approach for measuring the object's surface reflectivity values. This requires an understanding of how the image of the object forms on the camera sensor. Typically, in a structured light system, the following factors influence image formation: (*i*) the ambient light coming directly to the camera sensor with an intensity of L^{a}, (*ii*) the ambient light with an intensity of L^{o} reflected by the object with surface reflectivity of ρ, ρL^{o}, (*iii*) the projected light with an intensity of L^{p} reflected by the object, ρL^{p}, and (*iv*) the noise of the sensors I^{n}. Assuming the camera sensitivity is γ and the exposure time is t, the camera image can then be described as

$$I(x, y; t) = \gamma[L^{\mathrm{a}} + \rho L^{\mathrm{o}} + \rho L^{\mathrm{p}}] \times t + I^{n}. \tag{5}$$

If the projected light L^{p} is intense enough, we can assume that L^{a} and L^{o} are negligible in comparison. We also know that for a given pixel, γ and ρ are constants. If we then also assume that the LED light is approximately constant over time, then L^{p} is also a constant for each pixel. (Because binary patterns are projected, the micromirrors will be stationary as explained in Sec. 2.2.) Therefore, Eq. (5) becomes

$$I(x, y; t) = \gamma \rho L^{\mathrm{p}} \times t + I^{\mathrm{n}} = k(x, y) \times t + c(x, y). \tag{6}$$

For a stationary object, $k(x, y)$ can be determined by capturing a set of images of the object with different exposure times and fitting a line to the intensities of each pixel with linear regression. Because γ and L^{p} are known and controlled, $k(x, y)$ can be used to determine the approximate surface reflectivity $\rho(x, y)$ for the object at each imaged pixel. Theoretically, only two images are required to determine $\rho(x, y)$. However, because of noise, more images are desirable to increase the accuracy of the determination. Moreover, the camera pixels behave nonlinearly when saturated and any images that might be affected by camera sensor nonlinearities cannot be used to compute $\rho(x, y)$. Therefore, having multiple images spanning a wide range of exposure times ensures enough data for reflectivity determination after removing any nonlinear images.

With the surface reflectivity $\rho(x, y)$ now well approximated, a strategy can be formed for selecting the optimum exposure time for each pixel $t(x, y)$. Several images can then be taken, encompassing the range of $t(x, y)$ values determined, and the images blended together to yield data of maximized quality for 3-D computations.[12] However, in practice, a single exposure time for the whole image is desirable to speed

Fig. 3 Comparison of computer-generated binary patterns: (a) One of the SBM patterns and (b) one of the OPWM patterns.

up the measurement procedures. The remainder of the framework must outline criteria for selecting this single, optimum exposure time.

In optimizing image exposure for 3-D computations, it is crucial to avoid saturating the camera sensor in areas of high surface reflectivity without sacrificing fringe contrast in areas of low surface reflectivity.[12] In other words, a trade-off must be made between overexposing the brightest areas of a subject and losing the fringes in the darkest areas of a subject in shadow. Therefore, the best approach selects a single exposure time that results in an image where the subject's high-reflectivity regions come as close to saturated as possible without actually becoming saturated. This is the operating principle of this proposed automatic exposure method.

In the proposed method, the measured reflectivity values of the subject are first isolated from the background and then sorted from greatest to least as $\rho_1 \geq \rho_2 \geq \ldots \geq \rho_{n-1} \geq \rho_n$, where n is the total number of reflectivity values belonging to the subject. An index m into this ordered set is selected according to the criteria

$$m = \text{Round}(n \times P), \tag{7}$$

where P is a chosen percentage. The reflectivity value at this index, ρ_m, is inserted into Eq. (6), and the intensity value output of Eq. (6) is set to $I_{\max}$, a maximum desired pixel intensity value for the final image. This yields

$$I_{\max} = \gamma \rho_m L^{\text{p}} \times t + c_m. \tag{8}$$

Here, c_m is the intercept value from the linear regression solution for the pixel with reflectivity ρ_m. Because $c_m \ll I_{\max}$, we can assume the effect of c_m to be negligible. Therefore, solving for t, we have the prediction equation

$$t = \frac{I_{\max}}{\gamma \rho_m L^{\text{p}}}. \tag{9}$$

The predicted exposure time t, used in conjunction with the same values of γ and L^{p} used in its determination, yields an image with approximately the upper P percentage of subject pixels having intensities $I \geq I_{\max}$. When $I_{\max}$ is set to the saturation point of the camera sensor and P is chosen small enough to prevent data loss from saturation, Eq. (9) yields the optimum exposure time for 3-D measurement.

3 Experiments

We developed the 3-D measurement system shown in Fig. 4 to verify the proposed technique. It includes a high-speed complementary metal oxide semiconductor (CMOS) camera (Phantom v9.1) and a light-emitting diode (LED) DLP projector (Logic PD DLP LightCommander). Both the projector and camera are outfitted with the AF Nikkor 50-mm focal length lens adjusted to f/1.8 to minimize the effect of ambient light on the results. The projector has a resolution of 1024 × 768, and the LEDs are set at 100% brightness to further minimize the effect of ambient light. The camera resolution is adjusted to 1152 × 1152, and the gain is set at 1.00 to avoid amplifying the noise. The camera is triggered with a 5-V square pulse from a function generator (Tektronix AFG 3022B) triggered off the projector sync signal (this serves to amplify the projector signal).

We verify the exposure time optimization procedure by testing on it a diffuse white sculpture, as shown in Fig. 5. To determine the reflectivity values for the sculpture, it was

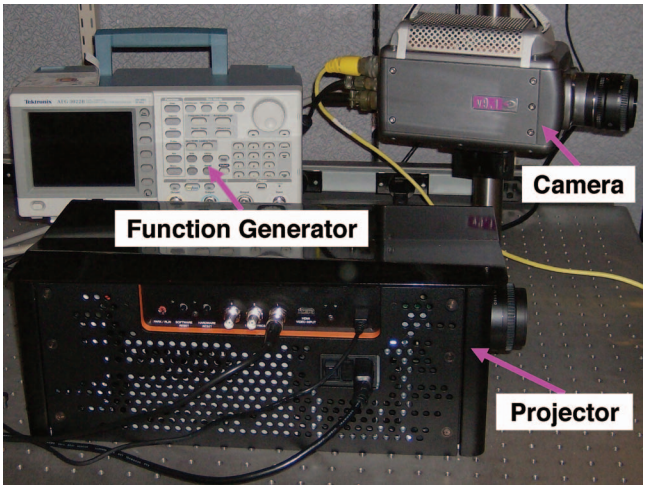

Fig. 4 Photograph of the test system.

photographed by the system camera against a black background under uniform pure white (255, 255, 255) illumination from the system projector. Photographs were taken at exposure times in increments of 50 μs from 50 to 700 μs. Figures 5(a)–5(d) contain four representative pictures from this set. From this image set, an optimized exposure time of 303 μs was predicted for the sculpture. Figure 5(e) shows the sculpture at its optimized exposure time, again illuminated by the projector with pure white light against a black background. This image appears to have the desired level of exposure for 3-D measurement. The sculpture's face is not overexposed, and although some details are lost in shadow, no facial details are underexposed.

To verify that this exposure time did indeed lead to good 3-D measurement results for the sculpture, the three-step phase-shifting algorithm was used to obtain 3-D data with the predicted exposure time of 303 μs. OPWM structured patterns were used to increase the measurement depth range, and the absolute phase maps were obtained through the multiwavelength technique.[13] Figure 5(f) shows a representative fringe image using the optimal exposure time and also shows that the fringe image has a good SNR for the sculpture's face. This results in the 3-D measurements of good quality shown in Fig. 5(g) and 5(h).

To further verify the proposed automatic exposure method, we test it on another sculpture, shown in comparison to the first in Fig. 6. This diffuse brown sculpture has a much lower average reflectivity value than the white one, and thus, it will require a much longer exposure time. Indeed, the automatic exposure algorithm predicted an exposure time of 1083 μs for this second sculpture when it was photographed under the same conditions as the first.

Figure 7 presents the representative fringe images and their corresponding 3-D measurement results for the two sculptures at these two predicted optimal exposure times (303 μs for the white sculpture and 1083 μs for the brown sculpture). Figures 7(a) and 7(b) are fringe images taken at t = 303 μs, and Figs. 7(e) and 7(f) are their resulting 3-D measurements. Compared to the high SNR and correct exposure of the white sculpture fringe image, the brown sculpture's fringe image has very low SNR and exhibits underexposed areas. This leads to the very poor 3-D measurement results for the brown sculpture shown in Fig. 7(f). Figures 7(c) and

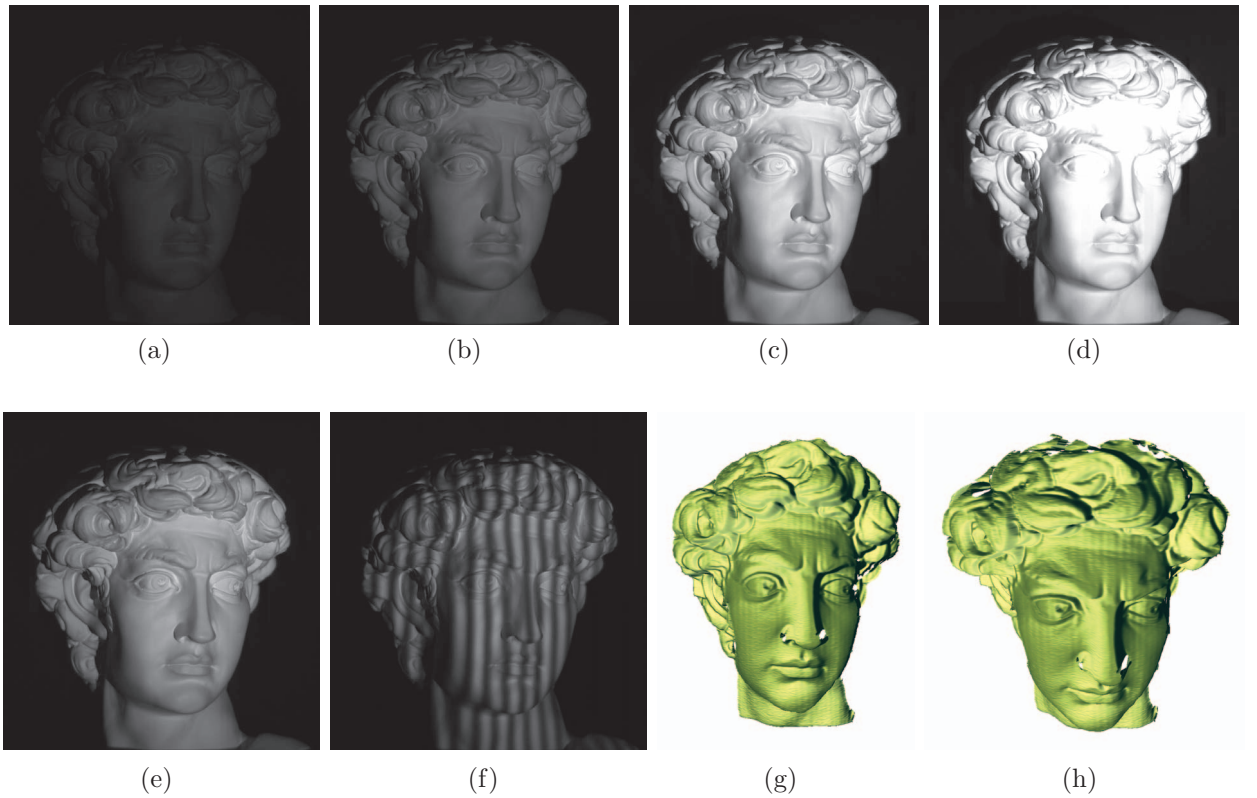

Fig. 5 Exposure time optimization process for a diffuse white sculpture. Reflectivity analysis images at exposure times of (a) 50 μs, (b) 150 μs, (c) 450 μs, and (d) 700 μs; (e) Sculpture at its predicted exposure time of 303 μs; (f) representative fringe image for $t = 303$ μs; and (g–h) 3-D measurement results for $t = 303$ μs.

7(d) are fringe images captured at $t = 1083$ μs, and Figs. 7(g) and 7(h) show their corresponding 3-D measurement results. Here, the white sculpture is very overexposed, whereas the brown sculpture has the correct exposure and good fringe SNR. The overexposure leads to incorrect measurement areas (depicted as large holes) in the 3-D measurement data shown in Fig. 7(g). However, as expected, the 3-D results for the brown sculpture in Fig. 7(h) are of high quality. This illustrates that the 3-D results for each sculpture are of good quality when the data are taken at their predicted optimal exposure time and are of very poor quality when the data are taken at a vastly different exposure time.

These experiments have demonstrated that the proposed automatic exposure time framework performs well. The framework is able to automatically determine the appropriate exposure time for high-quality 3-D shape measurement, successfully preventing the drastic errors caused by gross over- or underexposure in the fringe images.

Fig. 6 Photograph of the two sculptures used for verification.

4 Discussion

4.1 *Sensor Nonlinearity Considerations*

The proposed technology assumes that the camera image grayscale value is a linear function of exposure time for a non-saturated image. However, we found that the CMOS camera we used exhibits significantly nonlinear behavior when the image grayscale value rises above ~200. Figure 8 presents the results of a nonlinearity test performed with the set of images used to predict the correct exposure time for the white sculpture. Representative images from this set are shown in Figs. 5(a)–5(d). For this test, the goodness-of-fit parameter R^2 (the coefficient of determination) for a linear fit of grayscale value to exposure time was calculated for 306,765 camera pixels. These pixels were those remaining after excluding the pixels that were saturated or that had intensity values under 20 (i.e., severely underexposed pixels) in the 700-μs exposure time image. In this way, nonlinear behaviors in the pixel set due to saturation and extreme underexposure noise were removed.

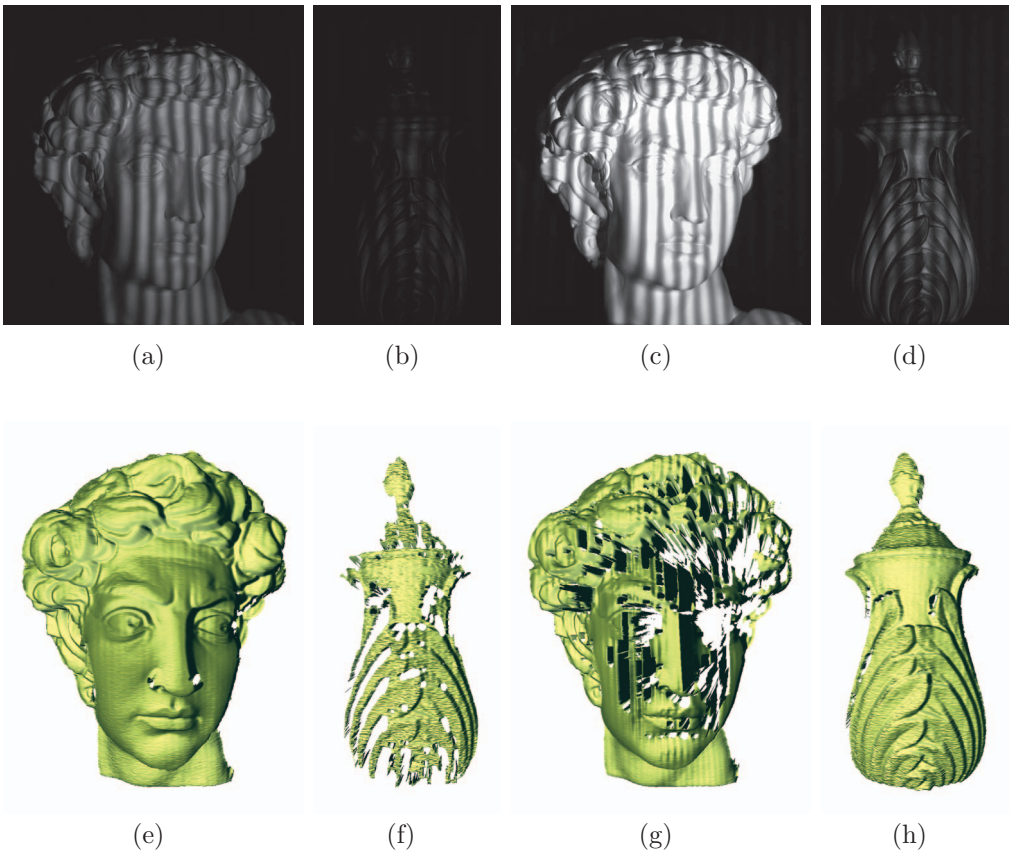

Fig. 7 Comparison of fringe images for the two sculptures and their resulting 3-D measurements. Representative fringe images for the sculptures at exposure times of (a, b) 303 μs and (c, d) 1083 μs, and (e–h) corresponding 3-D results.

Figure 8(a) presents a relative frequency histogram of the R^2 values for the 306,765 pixels. While ~70% of the pixels behave linearly, a significant percentage of the pixels exhibit nonlinear behavior. About 5% of the pixels have $R^2 = 0.995$, and the behaviors of four of these pixels with increasing exposure time are plotted in Fig. 8(b). Figure 8(b) shows that when the image grayscale value is under 200, the pixels exhibit reasonably linear behavior. However, beyond 200, the pixel behaviors are clearly nonlinear.

This nonlinearity affecting ~30% of the pixels leads to incorrect reflectivity predictions for those pixels, which in turn leads to an incorrect prediction of the optimized exposure

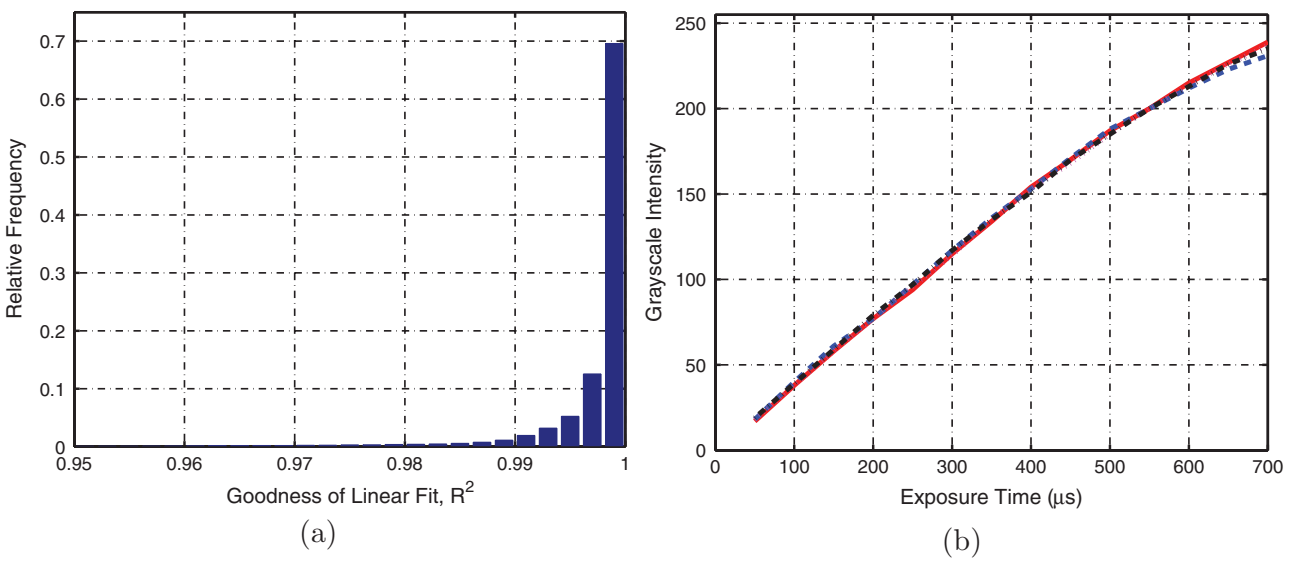

Fig. 8 CMOS sensor nonlinearity data: (a) Histogram of the goodness of linear fit parameter R^2 for 306,765 nonsaturated, nonshadowed pixels and (b) nonlinear behavior for four selected pixels with $R^2 = 0.995$.

time. This nonlinearity can also reduce the accuracy of the 3-D measurements. Therefore, for this research, images with grayscale values of >200 were not used to compute reflectivity values, and the optimized exposure time was computed by limiting the number of pixels allowed to reach a grayscale value of 200 rather than 255 in the final optimized image. This led to 3-D measurements of good quality as demonstrated above.

4.2 *Potential for High-Dynamic-Range Applications*

The automatic exposure technique has the potential to automate the high dynamic range scanning (HDRS) technique proposed by Zhang and Yau.[12] The HDRS technique captures each fringe image at multiple exposure levels to ensure that every region of the subject is photographed with good contrast for each fringe image. For an n-step phase-shifting algorithm, the multiple exposures are combined pixel by pixel into the required n fringe images in such a way that each pixel of the subject in the resulting images is at its brightest yet unsaturated exposure level. In this way, the HDRS technique can yield good quality 3-D profilometry for objects with a wide range of reflectivity values. The original HDRS technique requires physical aperture adjustments for each exposure level; and, even with a motorized aperture, these adjustments can cause undesired motion between fringe projection system components that alters the system calibration. The automatic exposure method could be adapted to perform the exposure adjustments for the HDRS method, making HDRS simpler and more versatile. However, integrating automatic exposure and HDRS will not prove straightforward because many difficult questions remain unanswered at this point. A framework must be developed to determine the optimal number of exposure levels needed for an object with arbitrary reflectivity values. The framework for the automatic exposure method must also be adapted to predict the multiple exposure times required for HDRS.

5 Conclusions

This paper has presented a framework for automatically adjusting image exposure to achieve high-quality 3-D measurements on a digital fringe projection system. The use of binary structured pattern defocusing techniques permits the system to have an arbitrary exposure time that can be used to automatically change the image intensity without sacrificing a good fringe signal-to-noise ratio. A series of images of the subject at increasing exposure times can be used to predict the correct exposure time for the subject. Experiments have shown that this predicted exposure time leads to good-quality 3-D results for the subject, avoiding the loss of data caused by over- and underexposure of the fringe images. This technique reduces the amount of human intervention required for 3-D measurement with digital fringe projection, allowing the system to be robust to changing diffuse subjects.

References

1. C. Waddington and J. Kofman, "Analysis of measurement sensitivity to illuminance and fringe-pattern gray levels for fringe-pattern projection adaptive to ambient lighting," *Opt. Laser Eng.* **48**, 251–256 (2010).
2. S. Lei and S. Zhang, "Digital sinusoidal fringe generation: defocusing binary patterns vs focusing sinusoidal patterns," *Opt. Laser Eng.* **48**(5), 561–569 (2010).
3. S. Lei and S. Zhang, "Flexible 3-D shape measurement using projector defocusing," *Opt. Lett.* **34**(20), 3080–3082 (2009).
4. Y. Wang and S. Zhang, "Optimum pulse width modulation for 3-D shape measurement with projector defocusing," *Opt. Lett.* **25**(24), 4121–4123 (2010).
5. Y. Gong and S. Zhang, "Ultrafast 3-D shape measurement with an off-the-shelf DLP projector," *Opt. Express* **18**(19), 19743–19754 (2010).
6. D. Malacara, Ed., *Optical Shop Testing*, 3rd ed, Wiley, Hoboken, NJ (2007).
7. D. C. Ghiglia and M. D. Pritt, *Two-Dimensional Phase Unwrapping: Theory, Algorithms, and Software*, Wiley, Hoboken, NJ (1998).
8. S. Zhang and P. S. Huang, "Novel method for structured light system calibration," *Opt. Eng.* **45**(8), 083601 (2006).
9. L. J. Hornbeck, "Digital light processing for high-brightness, high-resolution applications," *Proc. SPIE* **3013**, 27–40 (1997).
10. X.-Y. Su, W.-S. Zhou, G. von Bally, and D. Vukicevic, "Automated phase-measuring profilometry using defocused projection of a Ronchi grating," *Opt. Commun.* **94**(13), 561–573 (1992).
11. V. G. Agelidis, A. Balouktsis, and I. Balouktsis, "On applying a minimization technique to the harmonic elimination PWM control: the bipolar waveform," *IEEE Power Electron Lett.* **2**, 41–44 (2004).
12. S. Zhang and S.-T. Yau, "High dynamic range scanning technique," *Opt. Eng.* **48**(3), 033604 (2009).
13. Y. Wang and S. Zhang, "Superfast multifrequency phase-shifting technique with optimal pulse width modulation," *Opt. Express* **19**(6), 5143–5148 (2011).

Laura Ekstrand began the pursuit of her PhD in mechanical engineering at Iowa State University in January 2011. She graduated summa cum laude from Iowa State University in December 2010 with her BS in mechanical engineering. Currently, she is working with Dr. Song Zhang to improve the accuracy and versatility of 3-D high-speed optical profilometry systems. Her research interests include machine vision, visualization, optics education, and optical metrology.

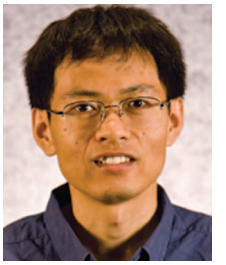

Song Zhang is an assistant professor of mechanical engineering at Iowa State University. He received his PhD in mechanical engineering from Stony Brook University in 2005 and worked as a postdoctoral fellow at Harvard University from 2005 to 2008. His major research interests include superfast 3-D optical metrology, biophotonic imaging, 3-D machine and computer vision, human computer interaction, and virtual reality. He serves as a reviewer for over a dozen journals.